Fluctuations in lifetime selection in an autocorrelated environment

Olivier Cotto, Luis-Miguel Chevin

FLUCTUATIONS IN LIFETIME SELECTION IN AN AUTOCORRELATED ENVIRONMENT

Olivier Cotto[1*] and Luis Miguel Chevin[1*]

1. Centre d'Ecologie Fonctionnelle et Evolutive Unité Mixte de Recherche 5175, Centre National de la Recherche Scientifique–Université de Montpellier, Université Paul-Valéry Montpellier, École Pratique des Hautes Études, 1919 route de Mende, 34293 Montpellier, Cedex 5, France.

Emails for correspondence *:

olivier.cotto2@gmail.com

luis-miguel.chevin@cefe.cnrs.fr

ABSTRACT

Most natural environments vary stochastically and are temporally autocorrelated. Previous theory investigating the effects of environmental autocorrelation on evolution mostly assumed that total fitness resulted from a single selection episode. Yet organisms are likely to experience selection repeatedly along their life, in response to possibly different environmental states. We model the evolution of a quantitative trait in organisms with non-overlapping generations undergoing several episodes of selection in a randomly fluctuating and autocorrelated environment. We show that the evolutionary dynamics depends not directly on fluctuations of the environment, but instead on those of an effective phenotypic optimum that integrates the effects of all selection episodes within

each generation. The variance and autocorrelation of the integrated optimum shape the variance and predictability of selection, with substantial qualitative and quantitative deviations from previous predictions considering a single selection episode per generation. We also investigate the consequence of multiple selection episodes per generation on population load. In particular, we identify a new load resulting from within-generation fluctuating selection, generating the death of individuals without significance for the evolutionary dynamics. Our study emphasizes how taking into account fluctuating selection within lifetime unravels new properties of evolutionary dynamics, with crucial implications notably with respect to responses to global changes.

INTRODUCTION

The study of adaptation to changing environments has received renewed attention in the context of current global changes induced by anthropogenic activities. Many theoretical studies on adaptation to changing environments have focused on cases where environmental change follows a deterministic trend (Lynch et al. 1991, Lynch and Lande 1993, Gomulkiewicz and Houle 2009, Cotto and Ronce 2014), motivated by major tendencies such as climate warming. Yet, most variation on short timescales results from stochastic fluctuations, and climatic time series generally include stochastic variations around their main trends (Stocker et al. 2013). The variance and autocorrelation of these fluctuations need to be modeled to accurately predict the impact of climate warming on biosystems (e.g. Katz 1996, Rowell 2005). Global climatic dynamics have recently been suggested to affect local selection pressures (Siepielski et al. 2017), and time series of climatic variables are generally autocorrelated in time, notably as a result of thermic inertia (Hasselmann 1976, Rowell 2005). As most climatic (and other ecologically relevant) environmental variables are autocorrelated in time (Vasseur and Yodzis 2004), environmental selective pressures are likely to also be temporally autocorrelated, an aspect that is often neglected in models of adaptation that do include stochasticity in the environment (e.g. Lynch and Lande 1993, Engen et al. 2011, Engen et al. 2012).

Theoretical models of adaptation to stochastically changing environments often assume that the fitness of an individual depends on the match between its phenotype and an optimum phenotype influenced by the environment (so-called “moving optimum” models, reviewed by Kopp and Matuszewski 2014). When the environment undergoes stationary stochastic fluctuations, the effect of evolutionary responses on long-term fitness and expected population growth depends on the variance and autocorrelation of changes in the optimum phenotype

(Charlesworth 1993, Lande and Shannon 1996, Chevin et al. 2017). If the stochastic fluctuations of the optimum are not autocorrelated, then responses to selection in a given generation might increase maladaptation in the next, with detrimental consequences for population growth (Lande and Shannon 1996). In contrast, temporal autocorrelation of the optimum makes the environment more predictable, such that the evolutionary response in a given generation is more likely to be beneficial in the next, and that any factor improving the response to selection leads to a higher expected long-term growth rate of the population (Lande and Shannon 1996, Chevin 2013). The autocorrelation of the optimum also affects the variance and overall shape of the probability distribution of population size of an evolving population, with consequences for extinction risk (Chevin et al. 2017). Lastly, temporal autocorrelation of the environment is a major driver of the evolution of plasticity, with higher reaction norm slopes evolving under more predictable (autocorrelated) environments of selection (Gavrilets and Scheiner 1993, Lande 2009, Chevin et al. 2015).

On the empirical side, a number of studies undertook to determine the temporal characteristics of selection in natural populations. Temporal variation in selection is observed in classic long-term surveys, like beak shape in Darwin's finches (Grant and Grant 2002), banding patterns in Cepea snails (Cain et al. 1990) or spine number in threespined sticklebacks (Reimchen and Nosil 2002, reviewed in Bell 2010). Consistent with these observations, studies analyzing several datasets with long-term selection estimates using a common framework also found that selection varies in strength and direction (Kingsolver and Diamond 2011, Siepielski et al. 2011, but see Morrissey and Hadfield 2012). Further, the development of a statistical framework that models temporal fluctuations in phenotypic selection as a random process, characterized by the variance and autocorrelation of an optimum phenotype, allowed to show that the optimum laying

77 date in a population of Great tits undergoes autocorrelated temporal fluctuations (Chevin et al.
78 2015, Gamelon et al. 2018). This framework rests on a model of a Gaussian fitness peak, as in
79 many theoretical studies (Kopp and Matuszewski 2014), so that the estimated parameters should
80 have a direct theoretical interpretation.

81 However, the comparison of empirical measures of fluctuating selection with theoretical
82 results on adaptation to autocorrelated environment is an arduous task, because the definitions of
83 fitness and selection may not be easily transposed from one to the other. Even regardless of
84 theoretical considerations about the definition of long-term expected fitness in a stochastic
85 environment, understanding how variation in selection integrates within lifetime is not
86 straightforward. Most theoretical studies that included autocorrelation in the environment
87 neglected the dynamics of selection within generations, by assuming (often implicitly) that
88 selection occurs instantaneously, in discrete non-overlapping generations. In other word, lifetime
89 fitness is assumed to result from a single instantaneous episode of selection; or at least, the
90 unfolding of selection within lifetime is not modeled explicitly, making it ambiguous whether the
91 per-generation optimum represents instantaneous or repeated selection. More realistically,
92 selection occurs in several episodes along a generation (Lande 1982, Arnold and Wade 1984b). In
93 fact, the vast majority of long-term estimates of selection gradients focused on a single fitness
94 component (~ 98% among 2819 selection estimates in Kingsolver and Diamond 2011), and
95 therefore correspond to a single episode of selection, among several possible others in a generation
96 or lifetime. This has several related consequences for the interpretation of measurements of
97 selection. First, the strength of selection over a single episode cannot necessarily be compared to
98 predictions based on overall selection per generation, because this selection episode needs to be
99 weighted by its contribution to the lifetime (or per-generation / per-unit-time) fitness. Second, both

100 the magnitude and predictability of temporal variation in selection is probably not well captured
101 by treating each selection episode in isolation. The reason is that in organisms that undergo
102 multiple selection episodes, environmental variability gets integrated over lifetime. This has
103 important consequences, notably regarding the contribution of extreme events to selection, a topic
104 of recent interest (Grant et al. 2017, Marrot et al. 2017).

105 The study of demography has long questioned the relationship between variation in vital
106 rates that contribute to elements of the transition matrix (e.g. fecundities, survival rates) and
107 various measures of the population growth rate (Tuljapurkar et al. 2003, Morris et al. 2004, Saether
108 et al. 2013). This theory has been used to analyse fluctuating selection in stochastic environments
109 that are not autocorrelated (Engen et al. 2012, 2014). However, how stochastic autocorrelated
110 fluctuating selection mediated by different fitness components integrates over lifetime is an under-
111 investigated topic, limiting our understanding of adaptation to randomly changing environments.
112 Making progress on this question requires extending previous approaches that integrate the
113 multiplicity of selection episodes along life. Of particular note is the approach by Arnold and Wade
114 (1984b, 1984a), who proposed and applied a decomposition of lifetime selection into a series of
115 selection episodes with multiplicative effects on fitness, resulting in selection gradients (dependent
116 on log-fitness) that sum along a generation (see also McGlothlin 2010). Integrating the effect of
117 successive selection episodes on lifetime fitness is appropriate to organisms with non-overlapping
118 generations (Arnold and Wade 1984a), but has not been used to investigate the effect of
119 environmental stochasticity.

120 We here build a model of a phenotypic trait exposed to multiple selection episodes, in non-
121 overlapping generations. We assume that the phenotype of an individual at the focal trait does not
122 change between selection episodes. This could correspond for example to a morphological trait

that only influences selection after it is fully developed, or a coloration trait that affects survival probability (due to e.g. predation, or thermoregulation) prior to reproduction. Under these assumptions, we detail and clarify how the temporal structure of selection during lifetime influences the predictability of lifetime viability selection, and the load caused by maladaptation in a stochastic environment. Our model applies directly to organisms that are semelparous with non-overlapping generations, including univoltine insects such as cicadas, and species with economic or cultural significance such as salmons or bamboos. Our analysis further applies to cohort analysis (see discussion) when considering more general life histories with overlapping generations. As such, our study provides a necessary step toward a complete understanding of how life history affects evolutionary dynamics in the context of autocorrelated fluctuating selection. Overall, we find that the way selection operates during a lifetime strongly determines the impact of environmental fluctuations on variation in selection across generations, and the incurred maladaptation load in a stochastic environment.

MODEL

Selection model

We investigate the evolution of a single quantitative trait z in an organism with non-overlapping generations. Along their life cycle, individuals undergo several selection episodes that determine their probability to survive between stages before reproduction, with the latter occurring only at the end of each generation. We further assume that there is no selection on fecundity, which we denote B. For simplicity, we focused on a single trait, but our framework can be readily extended to the multivariate case, with different (correlated) traits undergoing selection at different stages (Arnold and Wade 1984b, Arnold and Wade 1984a, Cotto and Ronce 2014).

We further assume that the phenotype *z* at the beginning of a generation can be decomposed as $z = x + e$, where *x* is the additive genetic value and *e* is a residual component of variation independent of the additive genetic value, and with normal distribution of mean 0 and variance *E* (Falconer and Mackay 1996). We assume that many loci contribute to the additive genetic value, such that *x* is normally distributed with mean $\bar{x}$ and variance *G*. Under these assumptions, *z* is also normally distributed with mean $\bar{z}$ and variance $P = G + E$.

The survival probability of an individual with phenotype *z* at age *i* in generation *g* depends on the match between its phenotype *z* and an optimum phenotype $\theta_{g,i}$ that changes with the environment,

$$W_{i,g}(z) = W_{max,i}\exp\left(-\frac{(z-\theta_{i,g})^2}{2\omega_{i,g}^2}\right). \quad (1)$$

where $W_{max,i}$ is the maximum survival rate at age *i* and ω_i measures the width of the Gaussian survival function (inversely related to the strength of selection). We assume that selection occurs through all transitions preceding reproduction, so that the components of fitness are multiplicative (Arnold and Wade 1984a). If reproduction could occur at several stages, then the components of fitness would no longer be multiplicative, and another framework (e.g. overlapping generations, Charlesworth 1994) should be used. The total absolute fitness of an individual with phenotype *z* is then (where the subscript *g* has been dropped for simplicity)

$$W(z) = B\prod_{i=1}^{n} W_i(z) \quad (2)$$

Under the assumption that selection is Gaussian at each episode (eq. 1), the total fitness function is also Gaussian,

$$W(z) = W_{max,tot}\exp\left(-\frac{(z-\theta_{tot})^2}{2\omega_{tot}^2}\right), \quad (3)$$

where, $\omega_{tot}^2 = (\sum_i 1/\omega_i^2)^{-1}$ is the total strength of selection (that is the harmonic mean of the width of the selection function at each selection episode), $\theta_{tot} = \sum_i e_i\,\theta_i$ is the per-generation effective optimum corresponding to the sum of the phenotypic optima at each selection episode, weighted by the contribution of these episodes to the total strength of selection. We denote this contribution as $e_i = \frac{\omega_{tot}^2}{\omega_i^2}$, by reference to elasticities in stage-structured population models (Caswell 2001). The maximum absolute fitness over a generation is

$$W_{max,tot} = B \exp\left(-\frac{1}{2\omega_{tot}^2}(\sum_i e_i\,\theta_i^2 - (\sum_i e_i\,\theta_i)^2)\right)\prod_i W_{max,i}. \quad (4)$$

With the further assumption that the strength of selection (here measured as a width of the fitness function) is the same at all selection episodes, we have $\omega_i = \omega$ and $e_i = 1/n$, so the equations above further simplify as

$$\omega_{tot}^2 = \omega^2/n \quad (5)$$

$$\theta_{tot} = \frac{1}{n}\sum_k \theta_k = \widehat{\mathrm{E}}[\theta] \quad (6)$$

$$W_{max,tot} = B \exp\left(-\frac{n\,\widehat{\mathrm{V}}[\theta]}{2\omega^2}\right)\prod_i W_{max,i}, \quad (7)$$

where $\widehat{\mathrm{E}}[\theta]$ and $\widehat{\mathrm{V}}[\theta]$ are the "sample" expectation and variance (respectively) of θ within a generation.

The change in the mean phenotype over an entire generation, after reproduction, is (Lande 1976)

$$\Delta\bar{z} = h_0^2(\bar{z}_n - \bar{z}_0) = G_0\frac{\partial \ln \overline{W}(z)}{\partial \bar{z}}, \quad (8)$$

where $\bar{z}_n$ is the mean phenotype after the last episode of selection, and additive genetic variance G_0 and heritability $h_0^2 = G_0/P_0$ are measured at the beginning of a generation, prior to any selection. Indeed, each selection event can generate a covariance between *P* and *E* that needs to be

accounted for if dealing with selection episode by episode (as in Arnold and Wade 1984a), resulting in complications (see Supp. Mat.) that can be overcome by focusing on the effect on total selection on the phenotype distribution prior to any selection. With Gaussian stabilizing selection (eq. 1) and a normally distributed trait, the mean fitness in the population is

$$\bar{W}(\bar{z}) = \int p(z)W(z)dz = W_{max,tot}\sqrt{S_{tot}\omega_{tot}^2}\exp\left(-\frac{(\bar{z}-\theta_{tot})^2}{2(\omega_{tot}^2+P_0)}\right), \quad (9)$$

where $S_{tot} = \frac{1}{P_0+\omega_{tot}^2}$. From equation 8, it follows that the per-generation change in the mean trait value in the population is

$$\Delta\bar{z} = -G_0 S_{tot}(\bar{z} - \theta_{tot}) = -G_0\beta_{tot}, \quad (10)$$

where β_{tot} is the total selection gradient, and which has a similar form as in models with a single selection episode (e.g. Lande 1976).

Fluctuations of the environment and timing of selection

We are interested in cases where the optimum phenotype fluctuates because of random fluctuations in the environment, i.e. fluctuations of the optimum phenotype represent those of the environment. For simplicity, we assume that the optimum phenotypes at all selection events in a life cycle respond to the same environmental variable, so that fluctuations in the optimum during a lifetime can be modeled as a temporal sampling of the same stochastic process. We consider the case where the optimum follows a first-order autoregressive process with mean 0 (without loss of generality), defined by

$$\theta_{t+1} = \rho\,\theta_t + \sigma_\theta\sqrt{1-\rho^2}\zeta_t \quad (11)$$

where ρ is the autocorrelation of the optimum over one (absolute; e.g. one year) time unit (which we assume is positive), σ_θ^2 its stationary stochastic variance, and ζ_t a standard normal random deviate. For such a process, the autocorrelation of the optimum over k units of time is $\rho^k =$

209 $\exp(-k/T_\theta)$, where $T_\theta = -1/\ln(\rho)$ is the characteristic timescale of the autocorrelation of the
210 optimum. Note that the autoregressive process converges to white noise when ρ tends to 0, i.e.
211 when the optimum phenotype is correlated over an infinitesimally small timescale.

212 We assume that *n* episodes of selection occur before reproduction. These selection episodes
213 all take place over a time-window that spans a fraction α of generation time *T*. The time-window
214 for selection remains unchanged across generations. This models the fact that all traits in an
215 organism need not be exposed to selection throughout life. Instead, it is more likely that there is a
216 time-window within a generation during which a given trait may be sensitive to the environment
217 and exposed to selection (e.g. during the first stages). When exactly the time-window of selection
218 occurs within a generation (e.g. at the beginning or at the end) has no effect for the remaining of
219 the analysis. Under our assumption of non-overlapping generations, only the duration of this
220 window matters. For simplicity, we assume that the episodes of selection are evenly spaced along
221 the time-window for selection, so that they occur every $\alpha T/n$ units of time. Using the index *g* for
222 the number of generations, we denote as $\bar{z}_{g,0}$ the mean trait value before the first episode of
223 selection of generation *g*. The timescale of life history relative to that of the environment is
224 represented in figure 1.

225 RESULTS

226 **Predictability of selection**

227 The predictability of selection can be defined in several ways. For our purpose, we will focus on
228 the autocorrelation of the effective optimum per generation, and that of the total selection gradient,
229 because these relate to measurable quantities (Lande and Arnold 1983, Chevin et al. 2015,
230 Gamelon et al. 2019) known to affect adaptation and population dynamics in a stochastic
231 environment (Lande and Shannon 1996, Chevin 2013, Chevin et al. 2017). We first calculate the

autocorrelation of θ_{tot}, before investigating the properties of the fluctuations in the selection gradient β_{tot}, which despite being less directly connected to theoretical predictions, are closer to what is commonly estimated empirically (Lande and Arnold 1983).

Autocorrelation of the effective optimum.

The autocorrelation of the effective optimum at a lag of one generation is (see also Supp. Mat.)

$$\rho_{\theta tot} = \rho^T \frac{\sum_{k=1}^{n} e_k^2 + \sum_{i=1}^{n-1} \sum_{j=i+1}^{n} e_i e_j \rho^{(j-i)\alpha T/n} \left(1+\rho^{2(i-j)\alpha T/n}\right)}{\sum_{k=1}^{n} e_k^2 + 2\sum_{i=1}^{n-1} \sum_{j=i+1}^{n} e_i e_j \rho^{(j-i)\alpha T/n}} = \rho^T \varphi, \quad (12)$$

where ρ^T is the autocorrelation of the optimum over a generation time, and its autocorrelation between two consecutive selection episodes is $\rho^{\alpha T/n}$ (which differs from the autocorrelation ρ per time-unit). In the following we detail the inflating factor φ corresponding to the complex fraction that appears in the first equality in equation (12). The first sum in the numerator results from the covariance between the optimum in a given episode of selection and the same episode in the next generation. The second sum results from the covariances of the optimum between two different selection episodes in two consecutive generations. The denominator has a similar structure, and results from similar effects (variance per episode *vs* covariance across episodes) within a generation, contributing to the variance of the effective optimum (see Supp. Mat.). It can be shown (by noting that $0 < \rho^{(j-i)\alpha T/n} \leq 1$, so that $\rho^{-(j-i)\alpha T/n} > 1$) that the ratio in equation (12) is always larger than 1, and is thus an inflating factor, which always increases the autocorrelation of the effective optimum relative to the autocorrelation of the environment, as a results of the averaging of selection between episodes within generations. Remarkably, this result extends to the autocorrelation over $\tau > 1$ generations when the autocorrelation of the environment decreases exponentially with time, as occurs under a Markovian process such as our first-order

autoregressive process. We thus have for the autocorrelation of the effective optimum over $\tau \geq 1$ generations

$$\rho_{\theta tot,\tau} = \rho^{\tau T}\varphi. \quad (13)$$

Equation (13) shows that, once the inflation factor has been accounted for, the autocorrelation of θ_{tot} declines exponentially at the same rate as the autocorrelation of θ (fig. 2A). In principle, then, information on the autocorrelation of the effective optimum between two generations allows to determine its autocorrelation over many generations, providing that the autocorrelation of the environment (here also corresponding to the autocorrelation of θ) driving selection is known.

More insights arise from the simpler case where the strength of selection is the same at all selection episodes (eq. 5-6), wherein φ simplifies to

$$\varphi = \frac{\psi+\psi^{-1}-2}{2(\psi-1)+n(\psi^{-\frac{1}{n}}-\psi^{\frac{1}{n}})}, \quad (14)$$

where $\psi = \rho^{\alpha T}$ is the autocorrelation of θ over the time window for selection. Equation (14) shows that when variance in the strength of stabilizing selection within generation can be neglected, then the inflation factor does not depend on the strength of selection, but only on environmental autocorrelation ψ over the time window for selection, and on the number of selection episodes. The inflation factor φ increases when the autocorrelation of the environment decreases (fig. 2B, C), and when the number of selection episode increases (fig. 2B). In other words, weakly autocorrelated environments can actually correspond to much larger autocorrelations of variables relevant to selection. For example, when there are many episodes of selection per generation and the autocorrelation of the environment is 0.2, the autocorrelation of θ_{tot} can be increased by more than 50% as compared to the autocorrelation of θ (fig. 2B). When the number of episodes of selection is large, φ converges to

$$\varphi \xrightarrow{n\to\infty} \frac{(1-\psi)^2}{2\psi(\psi-\ln\psi-1)}, \quad (15)$$

which only depends on environmental autocorrelation ψ over the time window for selection. We found that equation (15) provides a good approximation for equation (13) as soon as there are more than a few episodes of selection per generation, and even if the actual strength of selection varies across episodes (fig. 2B). Interestingly, equation (15) does not depend on the strength of selection at each episode, and proposes a simple transformation between the autocorrelation of the environment and the autocorrelation of the effective optimum over a generation time. Substituting equation (15) into equation (13) thus provides, in principle, a simple way to estimate the autocorrelation of the effective optimum in natural populations from a measure of the autocorrelation of the environment, over the duration of selection within a generation on one hand (to compute the inflation factor), and across generations on the other hand. The longer the organism is sensitive to selection within a generation, the larger the inflation factor (fig. 2C). Lastly, when the environment is not autocorrelated, the effective optimum is not autocorrelated either, showing that within-generation selection alone does not generate autocorrelation of the effective optimum.

Fluctuations in directional selection.

Variance of the selection gradient

Ultimately, evolutionary change in the mean phenotype in response to selection is directly related to the total per-generation selection gradient β_{tot} (eq. 10). At stationarity after many generations, we find that the variance of the selection gradient is approximately (see Supp. Mat.)

$$\mathrm{Var}[\beta_{tot}] \approx 2\,\mathrm{Var}[\theta_{tot}] S_{tot}^2 \frac{1-\rho^T\left(1+S_{tot}G_0(I_f-1)\right)}{(2-S_{tot}G_0)(1-\rho^T(1-S_{tot}G_0))}. \quad (16)$$

The variance of the selection gradient increases with the variance of fluctuations in the effective optimum (and of the environment, see Supp. Mat.) and with the total strength of selection (eq. 16 and fig. 3). Equation (16) further shows that the variance of the selection gradient decreases when the inflation factor increases. Correspondingly, $\mathrm{Var}[\beta_{tot}]$ decreases with α (because the inflation factor increases with α, fig. 2C) and with the number of selection episodes (fig. 2B and 3A). In other words, recurrent selection along a generation tends to decrease the variance of the selection gradient, as expected since environmental variation is averaged among selection episodes.

Less expected is the effect of environmental autocorrelation. We find that with several selection episodes per generation, the variance of the selection gradient depends non-monotonically on the autocorrelation of the environment, with a maximum when the environment is moderately autocorrelated (fig. 3B). This result contrasts with the case with a single selection episode per generation, where the variance in the selection gradient decreases with increasing autocorrelation of the environment, as a result of better adaptive tracking of the optimum (Lande and Shannon 1996, Chevin and Haller 2014). This difference arises because, with several episodes of selection, positive autocorrelation in the environment not only produces autocorrelation of the total optimum θ_{tot} across generations, but also increases the variance of θ_{tot} (see eq. A1 and fig. A1 in Supp. Mat.), with antagonistic effects on adaptive tracking by genetic evolution, and hence on the variance of the total selection gradient across generations (Lande and Shannon 1996, Chevin and Haller 2014).

We also investigated the influence of variable selection strength, by comparing the variance of the selection gradient obtained for a fixed strength of selection per episode (eq. 5-6) with the case where the strength of selection is drawn randomly at each episode from a distribution with the same expected total selection S_{tot} (details in fig. 2 caption). We found that when there are only few

episodes of selection per generation, variance in total selection per generation increases the variance of the selection gradient relative to what is expected in the deterministic case. However, with many selection episodes per generation, the variance in total selection decreases, resulting in a good fit between the simulations and the deterministic expectation (fig. 3, compare crosses with dashed lines and circles). The effect of random selection per generation increases when selection is strong (fig. 3). Lastly, we compared predictions from equation (16) calculated from a discrete generation model to previous results using a continuous time approximation (Lande and Shannon 1996 eq. 7 and table 1, and Chevin and Haller 2014 eq. 5a). The continuous time approximation provides more compact equations but tends to underestimate the variance of the selection gradient when selection increases (fig. 3, compare dashed and continuous lines).

Autocorrelation of the selection gradient

For the autocorrelation function of the total selection gradient across generations, we start by analyzing its expression in the case of a single selection episode per generation (i.e. when φ = 1). We obtain (see Supp. Mat.) for selection gradients τ generations apart

$$\rho_{\beta tot,\tau|n=1} = \frac{\rho^{\tau T} - \kappa(1 - S_{tot}\, G_0)^{\tau}}{1-\kappa}, \qquad (17)$$

where $\kappa \approx S_{tot}\, G_0 \frac{(1+\rho^T)}{2(1-\rho^T)}$ (see eq. A15). Equation (17) is similar in form to an expression obtained previously using a continuous-time approximation (eq. 5a in Chevin and Haller 2014), and leads to similar conclusions. The autocorrelation of the selection gradient with one selection episode is a linear combination of two exponentially decreasing functions, corresponding on the one hand to the autocorrelation of the environment (first term in numerator), and to evolutionary responses to

deviations from the optimum (second term in the numerator) on the other hand. Consistent with the result of Chevin and Haller (2014), we find that for large autocorrelation in the environment, equation (17) converges to $(1 - S_{tot}\, G_0)^{\tau}$, demonstrating that inertia in responses to selection sets an upper limit to the autocorrelation of the selection gradient.

In the general case where selection can occur in several episodes within a generation, we find a more complex expression for the autocorrelation of the selection gradient, which can nevertheless still be written in the form

$$\rho_{\beta tot,\tau} = \frac{\varphi\varepsilon\rho^{\tau T} + \gamma(1 - S_{tot}\, G_0)^{\tau}}{\vartheta}, \qquad (18)$$

where the detailed expressions of ε, γ and ϑ depend on the per-generation evolutionary potential $S_{tot}\, G_0$, the autocorrelation of the environment over a generation ρ^T, and γ and ϑ depend additionally on the inflation factor φ. The details of these terms can be found in the calculations provided in supplementary material (eq. A14). Equations (17) and (18) provide general expressions for the autocorrelation of the selection gradient with discrete generations and multiple selection episodes, extending previous results that used a continuous-time approximation with a single episode (Chevin and Haller 2014).

Comparing equations (17) and (18) highlights that with multiple selection episodes, the autocorrelation of the environment ρ and the rate of response to selection $S_{tot}\, G_0$ do not have in general an additive influence on the autocorrelation of selection gradients across generations, because the factor φ multiplying the former depends on the latter, and reciprocally for γ. This occurs because with multiple episodes of selection, the relevant autocorrelation is that of the effective optimum, which integrates the effect of selection across *and within* generations. The autocorrelation of the selection gradient increases most with the number of selection episodes when the autocorrelation of the environment is low (fig. 4A), consistent with what we found for

the inflation factor (fig. 2B and eq. 18). We also find that for a given number of selection episodes per generation, the autocorrelation of the selection gradient slightly decreases when the total strength of selection increases (fig. 4B).

Over time intervals longer than a generation, the autocorrelation function of selection gradients for a single selection episode (eq. 17) and for multiple episodes (eq. 18) have a similar shape (fig. 5), because they depend on the autocorrelation of the environment and of the effective optimum (respectively), which have the same exponential rate of decrease (fig. 2A). Importantly however, the autocorrelation of βtot in the first few generations - where the effect of multiple episodes is most pronounced - weights most in determining the expected maladaptation in a given generation (see e.g. eq. A6 in Supp. Mat.), so that differences in autocorrelation over short intervals of generations can have profound effects. It is worth mentioning that equations (17) and (18) can produce negative autocorrelations (fig. 5) when the effect of the evolutionary inertia (second term at the numerator) grows larger that the effect of the autocorrelation of environment (see also Chevin and Haller 2014).

Lastly, and similarly to the variance of the selection gradient, we found that when the strength of selection is drawn randomly at each selection episode (see previous related paragraph for variance), the autocorrelation of selection is below its expectation under constant selection strength, when there are only few selection episodes per generation (fig. 4A). This difference is especially marked when the environment is very autocorrelated and when selection is strong (fig. 4A, B) and vanishes as the number of selection episodes per generation increases.

Maladaptation load

Much of the work on adaptation of quantitative traits to autocorrelated stochastic environments has focused on the resulting expected lag load caused by deviations of the mean phenotype from the optimum, as this directly connects to long-term population growth and extinction risk (Lande and Shannon 1996, Chevin et al. 2017). From equation (10), the log mean fitness in the population (which relates to the relative increase in population size) is

$$\ln\overline{W} = r_{max} - \frac{1}{2\omega_{tot}^2}\left[\sum_k e_k\,\theta_k^2 - \left(\sum_k e_k\,\theta_k\right)^2\right] - \frac{1}{2}\ln\left(1+\frac{P_0}{\omega_{tot}^2}\right) - \frac{S_{tot}}{2}\left(\bar{z}-\theta_{tot}\right)^2 \qquad (19)$$

where $r_{max} = \ln B + \sum_{k=1}^{n} r_{max,k}$ corresponds to the maximum potential fitness, for a hypothetical population that would be monomorphic for the optimal phenotype in each selection episode. The last two terms describe reductions in fitness caused by maladaptation of the mean phenotype and phenotypic variance in the population, as described in the literature (Lande and Shannon 1996). When considering several selection episodes per generation, there is an additional load that is directly linked to the fluctuations in the optimum (second term in eq. 19). Indeed, this load vanishes when the optimum does not fluctuate across episodes ($\theta_k = \theta$ for all k). It thus corresponds to the deaths of individuals induced by environmental fluctuations within a generation, which reduce population growth without evolutionary significance. Note that when the trait has phenotypic variance, the mean phenotype does change under selection within a generation, tracking the optimum phenotype to some extent following each selection episode. But each of these selection episodes requires a number of selective deaths, and the resulting total cost of natural selection (sensu Haldane 1957) over a generation is unaffected by phenotypic tracking: the load is exactly the same if there is no phenotypic variation, and no within-generation phenotypic tracking. When the strength of selection at each episode ω is constant (corresponding to eq. 5), we further have

$$\frac{1}{2\omega_{tot}^2}\left[\sum_k e_k\,\theta_k^2 - \left(\sum_k e_k\,\theta_k\right)^2\right] = \frac{n\,\hat{\mathrm{V}}[\theta]}{2\omega^2}, \qquad (20)$$

such that the intra-generational load is proportional to the sample variance $\widehat{\mathrm{V}}[\theta]$ of the optimum across selection episodes within a generation.

In models of selection with a Gaussian fitness peak, there is a simple connection between the temporal distribution of the directional selection gradients and the expected maladaptation affecting populations growth, since both depend on the expected squared mismatch of the mean phenotype from the optimum (Chevin and Haller 2014), $y = \bar{z} - \theta_{tot}$. The expected maladaptation load L_m, defined as the decrease in log mean fitness induced by a mismatch between the population mean and the optimum phenotype, is $E[L_m] = \frac{S}{2}E[(\bar{z} - \theta_{tot})^2] = \frac{S}{2}\mathrm{Var}[y]$ in a stationary stochastic environment, and the variance of the selection gradient is $Var[\beta_{tot}] = S_{tot}^2 Var[y]$ (eq. A5), leading to the simple relationship $\mathrm{E}[L_m] = \mathrm{Var}[\beta_{tot}]/(2S_{tot})$. The maladaptation load in a fluctuating environment thus increases with the variance of the selection gradient and decreases with the total strength of selection. In particular, in an autoregressive environment where several selection episodes can occur within generations, we find that

$$\mathrm{E}[L_m] = \mathrm{Var}[\theta_{tot}] S_{tot} \frac{1-\rho^T\left(1+S_{tot}G_0\left(I_f-1\right)\right)}{(2-S_{tot}G_0)(1-\rho^T(1-S_{tot}G_0))} \qquad (21)$$

The first term in equation (21) shows that the expected component of the maladaptation load affected by responses to selection increases with the variance of the effective optimum (weighted by the strength of selection). The maladaptation load changes non-monotonically as a function of the autocorrelation of the environment (fig. 6A), as does the variance of the total selection gradient (fig 3A). Total maladaptation is strongest at intermediate autocorrelation of the environment (fig. 6A), contrary to the case of a single selection episode. Furthermore, the expected maladaptation decreases with increasing number of selection episodes within generation (fig. 6B), because this decreases the variance of the effective optimum, and in turn the variance of the selection gradient (see Supp. Mat. and fig. A1). However, note that this decreased variance of the effective optimum

come at the expense of an increased load of fluctuating selection within a generation, which cannot be overcome by adaptive tracking.

DISCUSSION

Most theoretical studies investigating the effect of an autocorrelated environment on evolutionary dynamics and their consequences for population dynamics assumed simple life cycles, where the timing of selection within a generation was left implicit (e.g. Charlesworth 1993, Lande and Shannon 1996, Chevin 2013). In models of non-overlapping generations, the timing of life-history events is generally not addressed, and selection is most often modeled as a single, effectively instantaneous process. This contrasts with the fact that many traits are likely to affect fitness at different times in life, and thus undergo several episodes of selection (Arnold and Wade 1984b, Marshall and Morgan 2011). Another difficulty at the interface of theory and empirical work on these questions is that measuring fitness is in practice challenging, such that natural selection is mostly estimated in the form of individual selection episodes acting via specific fitness components in the life cycle (Kingsolver and Diamond 2011, Siepielski et al. 2017). Recent refinements (e.g. McGlothlin 2010) of theory on the measurement of selection gradient (Lande and Arnold 1983, Arnold and Wade 1984a, Wade and Kalisz 1989) investigated how estimates of selection at different episodes within a generation can be integrated to infer overall selection, and the resulting evolutionary response. The present study extends this theory by investigating how fluctuating selection resulting from changes in the environment within and across generations impacts evolutionary trajectories, and the potential for population persistence.

To this aim, we developed a model of an organism with non-overlapping generations, where several transitions between stages (survival) prior to reproduction depend on the match

between a phenotypic trait and a fluctuating optimal value directly related to the environment, consistent with recent empirical estimates of fluctuating selection in the form of a moving phenotypic optimum (Chevin et al. 2015, Gamelon et al. 2019). Our analysis of this model demonstrates that knowledge of fluctuation patterns for the environment affecting selection is not sufficient to infer the predictability of selection across generations, when there are multiple selection episodes per generation. Selection across generations depends on an integrated optimum that includes the relative contribution of each selection episode to total selection along the life cycle, similar to recent formulations for age-structured populations but without autocorrelation (Engen et al. 2011, Cotto et al. 2019). Therefore, fluctuations of selection across generations depend on the pattern of variance and autocorrelation of the effective optimum, rather than of the environment *per se*. One of our main results is that, when the environment undergoes red noise (first-order autoregressive process), fluctuating selection within a generation causes the autocorrelation of the effective optimum to be inflated relative to the autocorrelation of the environment. We show that as the number of selection episode per generation increases, the inflation factor rapidly converges to an asymptotic value that depends neither on the number of episodes of selection nor on the strength of selection, but only on the autocorrelation of the environment over a time window of selection. This asymptotic value can be used in practical situations to estimate the autocorrelation of the effective optimum directly from measurement of the autocorrelation of the environment. Importantly, however, this result depends on the assumption that total selection (or its expectation) does not depend on the number of selection episodes per generation. This assumption allows us to disentangle the effect of selection acting repetitively along a generation from the effect of stronger total selection. We emphasize that this

independence may not be satisfied in natural populations, where more selection episodes may often cause stronger overall selection.

The inflation factor for the optimum directly influences the autocorrelation of directional selection gradients, which relates more directly to empirical measurements of the predictability and consistency of directional selection through time (Grant and Grant 2002, Morrissey and Hadfield 2012). However, an important point when considering the connection with empirical work is that, instead of tracking phenotypic change under selection episode per episode as done empirically (Arnold and Wade 1984b, McGlothlin 2010), we combined all episodes to derive a total per-generation individual fitness function. This allowed us to elude the difficulties arising from the dynamics of variances and covariances of breeding and phenotypic values at each successive episode of selection (see Supp. Mat. for the calculations per-episode). Indeed, the quantitative genetics framework assumes that genetic and environmental values are independent prior to selection. It is no longer the case after the first episode of selection within a generation (prior to reproduction), which generates a covariance between the above components. Tracking changes in the mean phenotype and breeding values across selection episodes therefore requires taking into account the change in covariance between breeding value and environmental values (See. Supp. Mat. for a demonstration). The buildup of this covariance complicates the investigation at the scale of individual selection episodes, from both a theoretical and empirical point of view (Wade and Kalisz 1989, Cam et al. 2002, McGlothlin 2010), because the selection gradients are no longer sufficient to describe accurately the change in the mean breeding value.

We also found that allowing for multiple selection episodes complicates the connection between environmental autocorrelation and the variance of selection gradients, which is directly linked to the expected maladaptation load reducing population growth (Chevin et al. 2017). With

multiple selection episodes, both these metrics vary non-monotonically with the autocorrelation of the environment, with a maximum at an intermediate value. This contrasts with previous results from models with a single episode of selection per generation, where the expected maladaptation load decreases monotonically with increasing autocorrelation of the environment, because this allows for closer adaptive tracking of the moving optimum via genetic evolution (Chevin 2013, Chevin et al. 2015). That this may not hold with multiple episodes of selection crucially revises previous understanding of the role of environmental autocorrelation on maladaptation: maladaptation can actually increase with increasing autocorrelation of the environment.

Lastly, we found that selection that fluctuates within a generation results in a specific load, which adds up to the maladaptation and variance loads classically described in the literature on adaptation to changing environments (see Lynch and Lande 1993, Burger and Lynch 1995, Lande and Shannon 1996, Kopp and Matuszewski 2014). This load only exists when the direction and/or strength of selection varies within a generation, and also increases with the number of selection episodes and the total per-generation strength of selection. The reason for this load is that each selection episode results in selective deaths that reduce the demographic output of the population, as previously discussed in extensions of Haldane's (1957) famous "cost of natural selection" to the context of adaptation to a changing environment, with a single selection episode (Nunney 2003). Within-generation fluctuations in selection increase this number of selective deaths without any net beneficial effect on adaptation: from an evolutionary perspective, individuals are essentially wasted by within-generation fluctuation in selection. An important implication of this result is that disturbances that increase temporal variation in the environment can lead to the decline of a population, regardless of its phenotypic state (mean phenotype, additive genetic variance). This bears particular importance in light of the increasing frequency of extreme climatic

events (Coumou and Rahmstorf 2012), and accumulating evidence of their effect on evolutionary and demographic dynamics (Moreno and Møller 2011, Marrot et al. 2017). This load caused by fluctuating selection within a generation may only be alleviated by mechanisms that cause within-generation adaptive changes in the mean phenotype without requiring any selective death. This suggests that a powerful mechanism by which labile, reversible plasticity can evolve (as investigated theoretically in a few studies, Gabriel 2005, Lande 2014, Ratikainen and Kokko 2019) is by reducing the load caused by fluctuating selection within a generation.

Our non-overlapping generation model applies directly to univoltine species. An interesting extension would be to investigate the case with overlapping generations. The most closely related life cycle with overlapping generations is that of perennial semelparous organisms, encompassing a large diversity of organisms (Young and Augspurger 1991) spanning from microbial parasites (Ebert and Weisser 1997) to long lived plants (e.g. semelparous yucca) and vertebrates (e.g. pacific salmon). This type of life cycle can lead to asynchrony in reproduction among age classes (Caswell 2001 p.81-88), such that the population at any time is composed of cohorts with different ages that rarely interbreed, in which case our conclusions directly apply to each of these cohorts. Perennial semelparous life cycles can also produce instability in age structure, which has been proposed to contribute to periodicity in species such as cicadas (Bulmer 1977) or bamboos (Keeley and Bond 1999). This instability may even lead to a collapse of age structure and to a synchrony in reproduction (Mjølhus et al. 2005), in which case our model would apply to the entire population. In contrast, iteroparity in perennial organisms would add considerable complications to the investigation of the effects of fluctuations in the environment. Indeed, each cohort of offspring is contributed from cohorts of reproductive individuals having

experienced different history of selection, possibly generating deviations from the stable (st)age structure (see Lorimer 1980 for an example). We leave such an investigation for a future study.

REFERENCES

Arnold, S. J., and M. J. Wade. 1984a. On the measurement of natural and sexual selection - theory. Evolution **38**:709-719.

Arnold, S. J., and M. J. Wade. 1984b. On the measurement of natural and sexual selection: applications. Evolution **38**:720-734.

Bell, G. 2010. Fluctuating selection: the perpetual renewal of adaptation in variable environments. Philos Trans R Soc Lond B Biol Sci **365**:87-97.

Bulmer, M. 1977. Periodical insects. The American Naturalist **111**:1099-1117.

Burger, R., and M. Lynch. 1995. Evolution and extinction in a changing environment: a quantitative-genetic analysis. Evolution:151-163.

Cain, A. J., L. Cook, and J. D. Currey. 1990. Population size and morph frequency in a long-term study of Cepaea nemoralis. Proc. R. Soc. Lond. B **240**:231-250.

Cam, E., W. A. Link, E. G. Cooch, J.-Y. Monnat, and E. Danchin. 2002. Individual covariation in life-history traits: seeing the trees despite the forest. The American Naturalist **159**:96-105.

Caswell, H. 2001. Matrix population models. Sinauer Associates Sunderland, Massachusetts, USA.

Charlesworth, B. 1993. Directional selection and the evolution of sex and recombination. Genetics Research **61**:205-224.

Charlesworth, B. 1994. Evolution in age-structured populations. Cambridge University Press Cambridge.

567 Chevin, L.-M., O. Cotto, and J. Ashander. 2017. Stochastic Evolutionary Demography under a
568 Fluctuating Optimum Phenotype. The American Naturalist **190**:786-802.
569 Chevin, L. M. 2013. Genetic constraints on adaptation to a changing environment. Evolution
570 **67**:708-721.
571 Chevin, L. M., and B. C. Haller. 2014. The temporal distribution of directional gradients under
572 selection for an optimum. Evolution **68**:3381-3394.
573 Chevin, L. M., M. E. Visser, and J. Tufto. 2015. Estimating the variation, autocorrelation, and
574 environmental sensitivity of phenotypic selection. Evolution **69**:2319-2332.
575 Cotto, O., and O. Ronce. 2014. Maladaptation as a source of senescence in habitats variable in
576 space and time. Evolution **68**:2481-2493.
577 Cotto, O., L. Sandell, L.-M. Chevin, and O. Ronce. 2019. Maladaptive Shifts in Life History in a
578 Changing Environment. The American Naturalist **194**:000-000.
579 Coumou, D., and S. Rahmstorf. 2012. A decade of weather extremes. Nature Climate Change
580 **2**:491.
581 Ebert, D., and W. W. Weisser. 1997. Optimal killing for obligate killers: the evolution of life
582 histories and virulence of semelparous parasites. Proceedings of the Royal Society of
583 London. Series B: Biological Sciences **264**:985-991.
584 Engen, S., R. Lande, and B. E. Saether. 2011. Evolution of a plastic quantitative trait in an age-
585 structured population in a fluctuating environment. Evolution **65**:2893-2906.
586 Engen, S., B. E. Saether, T. Kvalnes, and H. Jensen. 2012. Estimating fluctuating selection in age-
587 structured populations. J Evol Biol **25**:1487-1499.
588 Falconer, D., and T. Mackay. 1996. Introduction to quantitative genetics. 1996. Harlow, Essex,
589 UK: Longmans Green **3**.

590 Gabriel, W. 2005. How stress selects for reversible phenotypic plasticity. Journal of Evolutionary
591 Biology **18**:873-883.
592 Gamelon, M., Tufto, J., Nilsson, A. L., Jerstad, K., Røstad, O. W., Stenseth, N. C., & Sæther, B.
593 E. (2018). Environmental drivers of varying selective optima in a small passerine: A
594 multivariate, multiepisodic approach. Evolution, 72(11), 2325-2342.
595 Gamelon, M., S. J. Vriend, S. Engen, F. Adriaensen, A. A. Dhondt, S. R. Evans, E. Matthysen, B.
596 C. Sheldon, and B. E. Sæther. 2019. Accounting for interspecific competition and age
597 structure in demographic analyses of density dependence improves predictions of
598 fluctuations in population size. Ecology Letters.
599 Gavrilets, S., and S. M. Scheiner. 1993. The genetics of phenotypic plasticity. V. Evolution of
600 reaction norm shape. Journal of Evolutionary Biology **6**:31-48.
601 Gomulkiewicz, R., and D. Houle. 2009. Demographic and Genetic Constraints on Evolution.
602 American Naturalist **174**:E218-E229.
603 Grant, P. R., and B. R. Grant. 2002. Unpredictable evolution in a 30-year study of Darwin's finches.
604 Science **296**:707-711.
605 Grant, P. R., B. R. Grant, R. B. Huey, M. T. Johnson, A. H. Knoll, and J. Schmitt. 2017. Evolution
606 caused by extreme events. Phil. Trans. R. Soc. B **372**:20160146.
607 Haldane, J. B. S. 1957. The cost of natural selection. Journal of Genetics **55**:511.
608 Hasselmann, K. 1976. Stochastic climate models part I. Theory. tellus **28**:473-485.
609 Katz, R. W. 1996. Use of conditional stochastic models to generate climate change scenarios.
610 Climatic Change **32**:237-255.
611 Keeley, J. E., and W. J. Bond. 1999. Mast flowering and semelparity in bamboos: the bamboo fire
612 cycle hypothesis. The American Naturalist **154**:383-391.

613 Kingsolver, J. G., and S. E. Diamond. 2011. Phenotypic selection in natural populations: what
614 limits directional selection? The American Naturalist **177**:346-357.
615 Kopp, M., and S. Matuszewski. 2014. Rapid evolution of quantitative traits: theoretical
616 perspectives. Evolutionary Applications **7**:169-191.
617 Lande, R. 1976. Natural selection and random genetic drift in phenotypic evolution. Evolution
618 **30**:314-334.
619 Lande, R. 1982. A quantitative genetic theory of life history evolution. Ecology:607-615.
620 Lande, R. (2007). Expected relative fitness and the adaptive topography of fluctuating selection.
621 Evolution, 61(8), 1835-1846.
622 Lande, R. 2009. Adaptation to an extraordinary environment by evolution of phenotypic plasticity
623 and genetic assimilation. Journal of Evolutionary Biology **22**:1435-1446.
624 Lande, R. 2014. Evolution of phenotypic plasticity and environmental tolerance of a labile
625 quantitative character in a fluctuating environment. J Evol Biol **27**:866-875.
626 Lande, R., and S. J. Arnold. 1983. The measurement of selection on correlated characters.
627 Evolution **37**:1210-1226.
628 Lande, R., and S. Shannon. 1996. The role of genetic variation in adaptation and population
629 persistence in a changing environment. Evolution **50**:434-437.
630 Lorimer, C. G. 1980. Age structure and disturbance history of a southern Appalachian virgin forest.
631 Ecology **61**:1169-1184.
632 Lynch, M., W. Gabriel, and A. M. Wood. 1991. Adaptive and demographic responses of plankton
633 populations to environmental-change. Limnology and Oceanography **36**:1301-1312.
634 Lynch, M., and R. Lande. 1993. Evolution and extinction in response to environmental change.
635 Biotic interactions and global change:234-250.

636 Marrot, P., D. Garant, and A. Charmantier. 2017. Multiple extreme climatic events strengthen
637 selection for earlier breeding in a wild passerine. Phil. Trans. R. Soc. B **372**:20160372.
638 Marshall, D. J., and S. G. Morgan. 2011. Ecological and evolutionary consequences of linked life-
639 history stages in the sea. Current Biology **21**:R718-R725.
640 McGlothlin, J. W. 2010. Combining selective episodes to estimate lifetime nonlinear selection.
641 Evolution **64**:1377-1385.
642 Mjølhus, E., A. Wikan, and T. Solberg. 2005. On synchronization in semelparous populations.
643 Journal of Mathematical Biology **50**:1-21.
644 Moreno, J., and A. P. Møller. 2011. Extreme climatic events in relation to global change and their
645 impact on life histories. Current Zoology **57**:375-389.
646 Morris, W. F., & Doak, D. F. (2004). Buffering of life histories against environmental
647 stochasticity: accounting for a spurious correlation between the variabilities of vital rates
648 and their contributions to fitness. The American Naturalist, 163(4), 579-590.
649 Morrissey, M. B., and J. D. Hadfield. 2012. Directional selection in temporally replicated studies
650 is remarkably consistent. Evolution **66**:435-442.
651 Nunney, L. 2003. The cost of natural selection revisited. Pages 185-194 *in* Annales Zoologici
652 Fennici. JSTOR.
653 Ratikainen, I. I., and H. Kokko. 2019. The coevolution of lifespan and reversible plasticity. Nature
654 Communications **10**:538.
655 Reimchen, T., and P. Nosil. 2002. Temporal variation in divergent selection on spine number in
656 threespine stickleback. Evolution **56**:2472-2483.
657 Rowell, D. P. 2005. A scenario of European climate change for the late twenty-first century:
658 seasonal means and interannual variability. Climate Dynamics **25**:837-849.

659 Engen, S., Sæther, B. E., Kvalnes, T., & Jensen, H. (2012). Estimating fluctuating selection in age-
660 structured populations. Journal of evolutionary biology, 25(8), 1487-1499.
661 Engen, S., Kvalnes, T., & Sæther, B. E. (2014). Estimating phenotypic selection in age-structured
662 populations by removing transient fluctuations. Evolution, 68(9), 2509-2523.
663 Engen, S., Sæther, B. E., Armitage, K. B., Blumstein, D. T., Clutton-Brock, T. H., Dobson, F. S.,
664 Festa-Bianchet, M., Oli, M. K. , Ozgul, A. (2013). Estimating the effect of temporally
665 autocorrelated environments on the demography of density-independent age-structured
666 populations. Methods in Ecology and Evolution, 4(6), 573-584.
667 Siepielski, A. M., J. D. DiBattista, J. A. Evans, and S. M. Carlson. 2011. Differences in the
668 temporal dynamics of phenotypic selection among fitness components in the wild.
669 Proceedings of the Royal Society of London B: Biological Sciences **278**:1572-1580.
670 Siepielski, A. M., M. B. Morrissey, M. Buoro, S. M. Carlson, C. M. Caruso, S. M. Clegg, T.
671 Coulson, J. DiBattista, K. M. Gotanda, and C. D. Francis. 2017. Precipitation drives global
672 variation in natural selection. Science **355**:959-962.
673 Stocker, T. F., D. Qin, G.-K. Plattner, M. Tignor, S. K. Allen, J. Boschung, A. Nauels, Y. Xia, V.
674 Bex, and P. M. Midgley. 2013. Climate change 2013: The physical science basis.
675 Cambridge University Press Cambridge.
676 Tuljapurkar, S., Horvitz, C. C., & Pascarella, J. B. (2003). The many growth rates and elasticities
677 of populations in random environments. The American Naturalist, 162(4), 489-502.
678 Vasseur, D. A., and P. Yodzis. 2004. The color of environmental noise. Ecology **85**:1146-1152.
679 Wade, M. J., and S. Kalisz. 1989. The additive partitioning of selection gradients. Evolution
680 **43**:1567-1569.

681 Young, T. P., and C. K. Augspurger. 1991. Ecology and evolution of long-lived semelparous
682 plants. Trends in Ecology & Evolution **6**:285-289.

683

684 FIGURE CAPTIONS

685

686 Figure 1: Schematic representation of the timescales and autocorrelation measures. Generations
687 last T units of time, within which selection occurs in n selection episodes spread over αT units of
688 time. The autocorrelation of the optimum phenotype (which is identical to that of the environment)
689 over the within-generation time of selection is $\psi = \rho^{\alpha T}$, and over a generation time is ρ^{T}. The per-
690 generation effective optimum integrates the effect of selection within generations. We denote $\rho_{\theta_{tot}}$
691 the autocorrelation of this measure over a generation. The schema highlights that the variance and
692 autocorrelation differ between the optimum phenotype at each episode of selection (i.e. the
693 environment) and the effective optimum relevant for the evolutionary dynamics across
694 generations.

695

696 Figure 2: Autocorrelation of the effective optimum and inflation factor. Panel A: Autocorrelation of the effective
697 optimum as a function of the number of generations for 10 selection episodes per generation. Panel B: Inflation factor
698 as a function of the number of selection episodes. Panel C: Inflation factor as a function of the duration of the selection
699 window relative to the generation time α. Dotted lines (panel A) correspond to the autocorrelation of the environment
700 (θ) alone over g generations: ρ^{gT}.Crosses show results from simulations with a strength of stabilizing selection that
701 varies across selection episodes, while lines show the expectation assuming constant selection strength with same
702 mean (full lines: exact prediction using eq. 12, dashed lines: prediction for continuous selection along each generation
703 – infinite number of selection episodes, eq. 15). Numerical simulations are performed using eq. (10), with θ_{tot} and
704 ω_{tot}^2 calculated as described in eq. 3 from phenotypic optima θ_i and corresponding strengthes of selection ω_i^2
705 corresponding to each episode of selection *i* per generation as described in the following: for each episode of selection,
706 a phenotypic optimum is drawn from equation 11 and the strength of selection is drawn independently in a Gaussian
707 with mean $\sqrt{\omega_{tot}^2/n - 1}$ and variance 1. Total selection per generation thus follows a non-central χ^2 with mean ω_{tot}^2
708 and variance $4\omega_{tot}^2 - 2n$. For simulations, we kept the expected total strength of selection constant (independent on
709 the number of selection episode) to isolate the effect of the number of selection episodes from that of the total strength

of selection. For A and B, α = 0.8. For all panels: light gray to black: $\rho^T = 0.2$, 0.5 and 0.9 respectively, $\bar{\omega}_{tot}^2$ = 25, $\sigma_\theta^2 = 1$.

Figure 3: Variance of the selection gradient as a function of the number of selection episode per generation (A) and of the autocorrelation of the environment (B). Panel A: environmental autocorrelation over a generation time is $\rho^T = 0.5$ (dark gray) and $\rho^T = 0.2$ (light gray), for two total strengths of selection per generation ($\bar{\omega}_{tot}^2$ = 25 [lower two sets of simulations/expectations] and 10 [upper sets]). Panel B represents the variance of the total selection gradient as a function of the autocorrelation of the environment, for the same two total strengths of selection, and n = 10. Crosses represent results from numerical simulations where the strength of stabilizing selection varies across selection episodes, whereas circles represent constant strength of stabilizing selection, as described in the caption of figure 2. The dashed lines correspond to the predictions from eq. (16). Continuous lines represent predictions derived from a continuous time approximation as in Lande and Shannon (1996, eq. 7), resulting in equation 5a in Chevin and Haller (2014): $\mathrm{Var}[\beta_{tot}] = \mathrm{Var}[\theta_{tot}]S_{tot}^2 \,/(1 + S_{tot}G_0T_\theta)$, where T_θ is the characteristic time scale of the autocorrelation of the environment (from eq. 13, and see eq. 11 and below). For both panels: α = 1 and $\sigma_\theta^2 = 1$.

Figure 4: Autocorrelation of βtot over a single generation as a function of the number of selection episodes (A) and of the total strength of selection per generation ω_{tot}^2 (B). Crosses represent results from numerical simulations with variable strength of stabilizing selection, whereas circles represent those with constant stabilizing selection, as described in the caption of figure 2. Dashed lines: expectations using equation 18. Continuous lines: expectation for a single selection episode (eq. 17). From light gray to black, ρ^T = 0.1, 0.5 and 0.9. Panel A: $\omega_{tot}^2 = 10$. Panel B: n = 5. For both panels: α = 1 and $\sigma_\theta^2 = 1$.

Figure 5: Autocorrelation function of βtot across generations. The embedded graph shows a detailed view of the first five generations. Crosses represent results from numerical simulations with variable strength of stabilizing selection whereas circles represent those with constant stabilizing selection, as described in the caption of figure 2. Dashed lines: expectations using equation (18). Continuous lines: expectation for a single selection episode (eq. 17). Note that for parameters shown here (number of selection episode and strength of selection) there is almost no difference

between simulations with deterministic (circles) and random (square) strength of selection per episode. From light gray to black, ρ^T = 0.1, 0.5 and 0.9, $\omega_{tot}^2 = 10$, α = 1 and $\sigma_\theta^2 = 1$.

Figure 6: Maladaptation load as a function of the autocorrelation of the environment ρ^T (A) and as a function of the number of selection episodes (B). Crosses represent results from numerical simulations with variable strength of stabilizing selection whereas circles represent those with constant stabilizing selection, as described in the caption of figure 2. The gray scale represents different number *n* of selection episodes per generation in panel A, and different autocorrelation of the environment in panel B (light to dark gray, $\rho^T = 0.2$, 0.5 and 0.9). For both panels, $\bar{\omega}_{tot}^2 = 25$, $\sigma_\theta^2 = 1$, $\alpha = 1$.

748 FIGURES

749

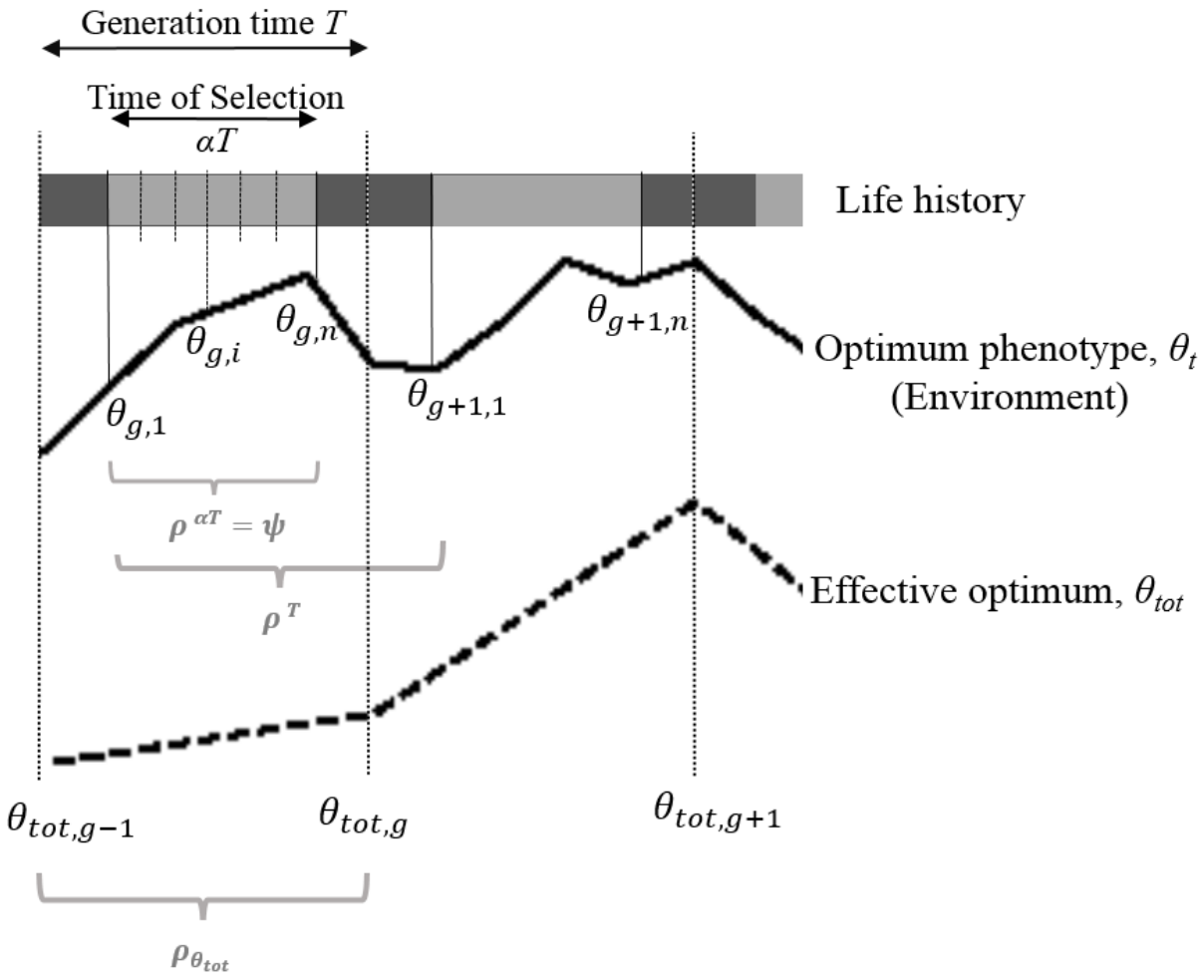

750

751 Figure 1

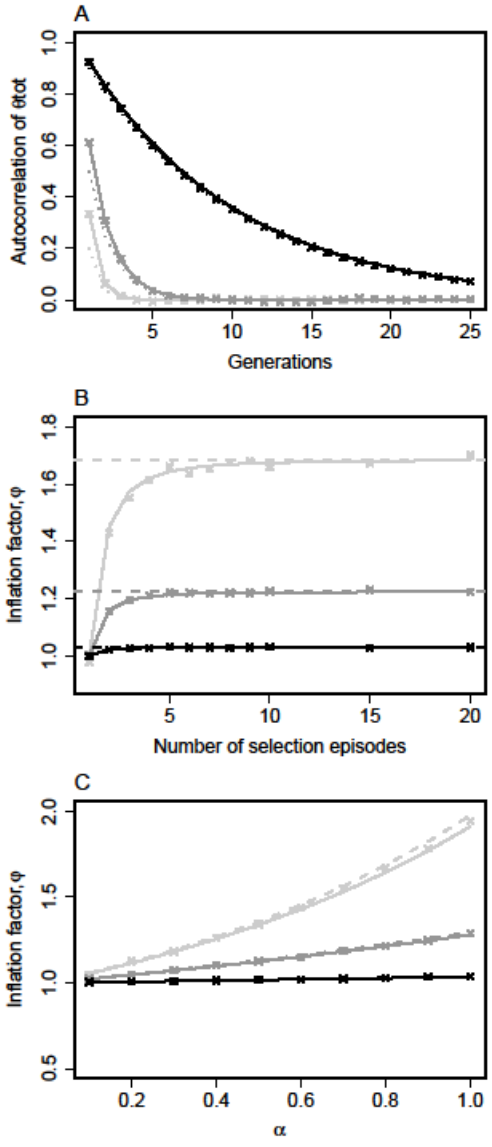

752

753 Figure 2

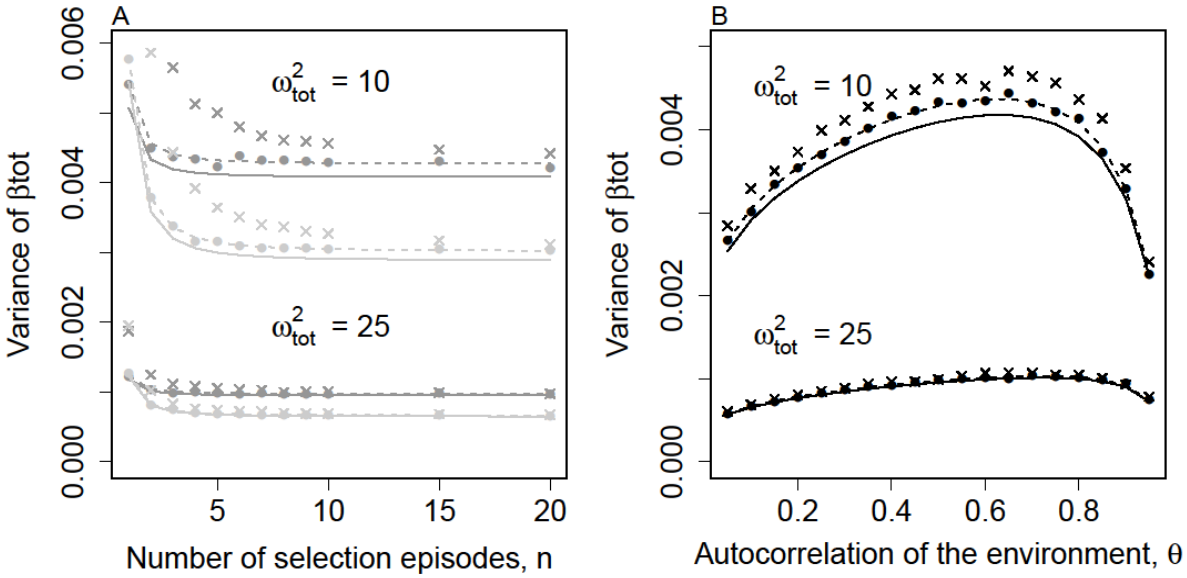

754

755 Figure 3

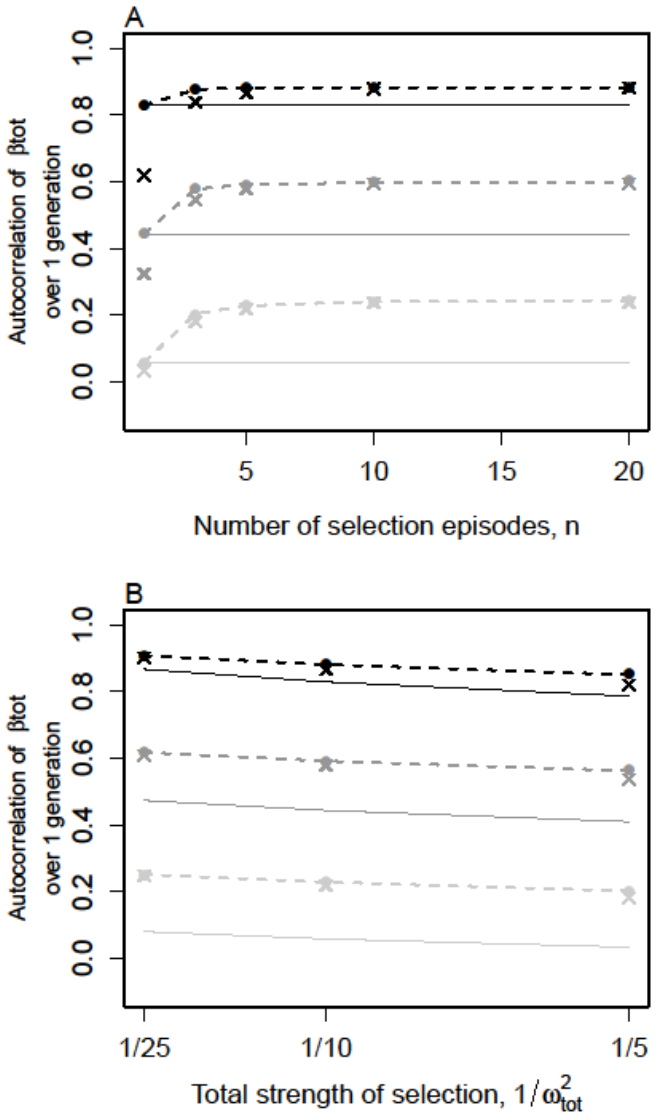

756

757 Figure 4

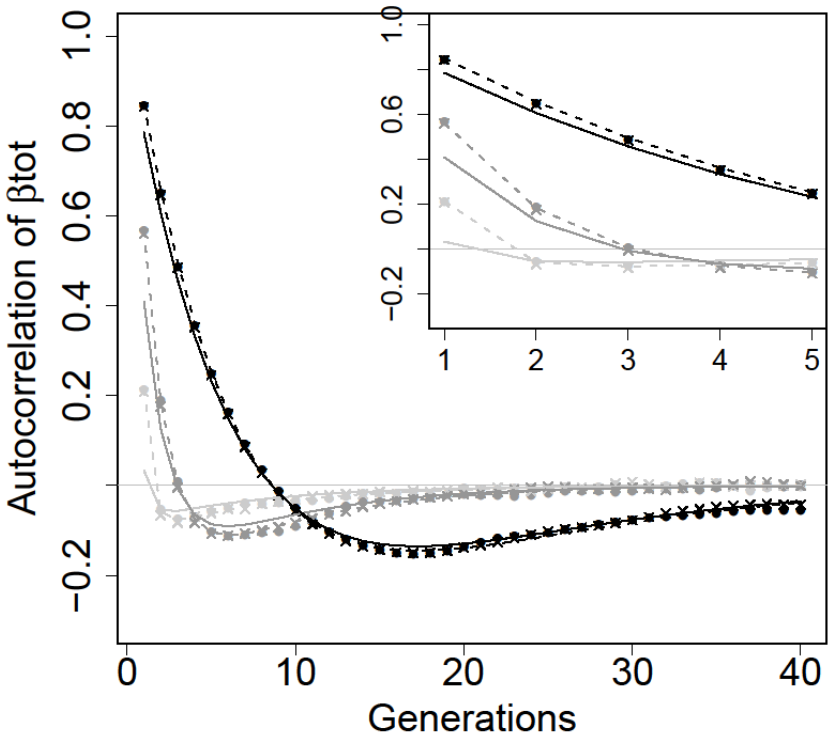

758

759 Figure 5

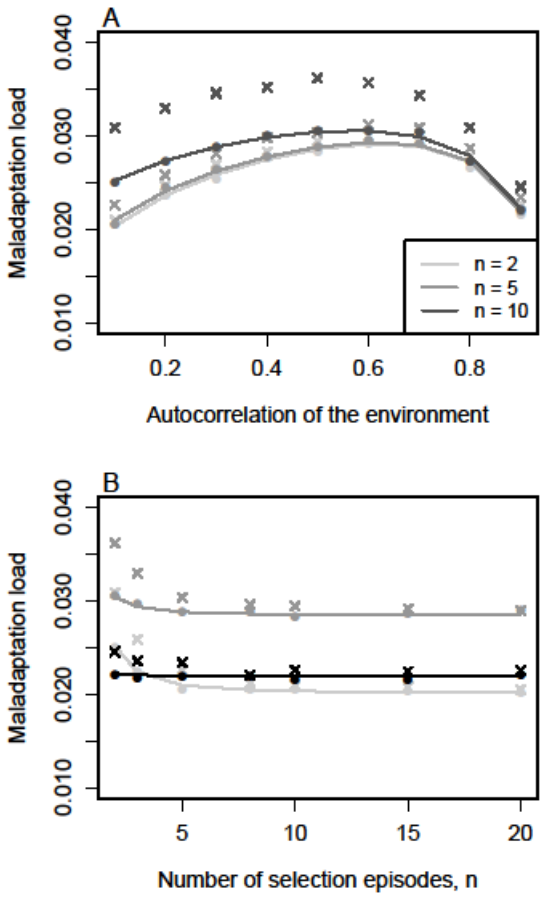

760

761 Figure 6

762

SUPPLEMENTARY ANALYSIS

Variance of the effective optimum

By definition, the variance in the per-generation effective optimum is

$$\mathrm{Var}[\theta_{tot}] = Var[\sum_{k=1}^{n} e_k\theta_k] = \sigma_\theta^2 \sum_{k=1}^{n} e_k^2 + 2\sum_{i=1}^{n-1}\sum_{j=i+1}^{n} cov\left[e_i\theta_i, e_j\theta_j\right], \quad \text{(A1)}$$

where σ_θ^2 is the stationary variance of the per-episode optimum. Rewriting (A1) using the properties of the autocorrelation of the environment (eq. 11) leads to

$$\mathrm{Var}[\theta_{tot}] = \sigma_\theta^2(\sum_{k=1}^{n} e_k^2 + 2\sum_{i=1}^{n-1}\sum_{j=i+1}^{n} e_i e_j \rho^{(j-i)\alpha T/n}), \quad \text{(A2)}$$

with $e_i = \omega_{tot}^2/\omega_i^2$. The first term in the right-hand side of equation (A2) corresponds to the direct contribution of the variance of the environment. The second term on the right-hand side results from the autocorrelation of the environment between selection episodes within a generation, generating additional variation to the effective optimum. With the further assumption that the strength of selection is the same at all episodes of selection, $\omega_i^2 = \omega^2$, Equation A2 further simplifies in

$$\mathrm{Var}[\theta_{tot}] = \sigma_\theta^2\left(\frac{1}{n} + \frac{2}{n}\sum_{i=1}^{n-1}\sum_{j=i+1}^{n}\rho_\theta^{(j-i)\alpha T/n}\right) = \sigma_\theta^2\frac{n - n\rho^{2\alpha T/n} + 2\rho^{\alpha T/n}(\rho^{\alpha T} - 1)}{n^2(\rho^{\alpha T/n} - 1)^2} \quad \text{(A3)}$$

The variance of the effective optimum θ_{tot} is always lower than the variance of the environment (set to 1 in figure A1), and decreases with increasing number of selection episodes (fig A1-A). However, $\mathrm{Var}[\theta_{tot}]$ does not decrease without bounds, instead reaching a limit value for a large number of episodes of selection, $\lim_{n\to\infty}(\mathrm{Var}[\theta_{tot}]) = 2\frac{\psi - \ln\psi - 1}{(\ln\psi)^2}$, which only depend on the autocorrelation of the environment over the time window for selection $\psi = \rho^{\alpha T}$. In addition, for a given number of selection episodes, the variance of the effective optimum increases with the autocorrelation of the environment (fig. A1-B).

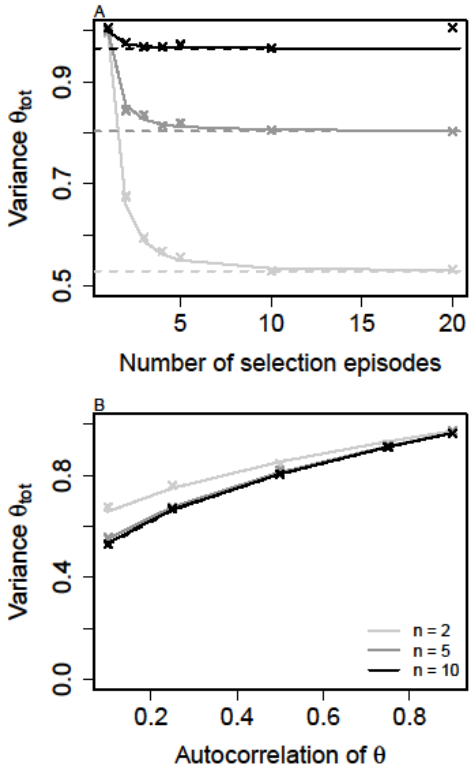

Figure A1: Variance of the effective optimum as a function of the number of selection episodes (A) and as a function of the autocorrelation of the environment (B). Crosses represent the results from simulations where the strength of selection is drawn from a probability distribution as described in fig. 2 caption. Full lines represent the expectation from eq. A3 and dashed lines represent the limit for a large number of selection episodes. Panel A: from light grey to dark $\rho_{\theta,T} = 0.2$, 0.5 and 0.9 respectively. Panel B: the gray scale represents different number of selection episode per generation (see within the panel). For both panels, $\bar{\omega}_{tot}^2 = 25$, $\sigma_\theta^2 = 1$, $\alpha = 1$.

Variance of the selection gradient

The variance of β_{tot} is proportional to the variance of the distance of the mean phenotype to the optimum

$$\mathrm{Var}[\beta_{tot}] = (S_{tot})^2 \mathrm{Var}[(\bar{z} - \theta_{tot})] = (S_{tot})^2 \mathrm{E}[(\bar{z} - \theta_{tot})^2]. \quad \text{(A4)}$$

By rearranging equation 10 in the main text (Charlesworth 1993), the mean phenotypic value at generation g is

$$\bar{z}_g = (1 - S_{tot}G_0)^g \bar{z}_0 + S_{tot}G_0 \sum_{i=1}^{g} (1 - S_{tot}G_0)^{i-1} \theta_{tot,g-i}. \quad \text{(A5)}$$

After a sufficiently large number of generations, the first term in equation (A5), corresponding to the initial conditions, can be neglected. We thus obtain

$$\mathrm{E}[(\bar{z} - \theta_{tot})^2] = \mathrm{E}\left[\left(S_{tot}G_0 \sum_{i=1}^{g} (1 - S_{tot}G_0)^{i-1} \theta_{tot,g-i} - \theta_{tot,g}\right)^2\right], \quad \text{(A6)}$$

By developing terms, using the autocorrelation of the effective optimum (eq. 12) and assuming that $g \to \infty$, we obtain equation (16) in the main text (see also Charlesworth 1993; eq. 19a)

$$\mathrm{Var}[\beta_{tot}] = 2\mathrm{Var}[\theta_{tot}] S_{tot}^2 \frac{1-\rho\left(1+S_{tot}G_0(\varphi-1)\right)}{(2-S_{tot}G_0)(1-\rho(1-S_{tot}G_0))}.$$

Autocorrelation of the selection gradient

The autocovariance of the selection gradient over τ generations is

$$\mathrm{Cov}\left[\beta_{tot,g}, \beta_{tot,g-\tau}\right] = S_{tot}^2\left(\mathrm{E}\left[\theta_{tot,g}\theta_{tot,g-\tau}\right] + \mathrm{E}\left[\bar{z}_g\bar{z}_{g-\tau}\right] - \mathrm{E}\left[\bar{z}_{g-\tau}\theta_{tot,g}\right] - \mathrm{E}\left[\theta_{tot,g-\tau}\bar{z}_g\right]\right). \quad \text{(A7)}$$

Continuous time approach

Following Lande and Shannon (1996), the dynamics can be approximated in continuous time. The continuous time approximation eases the analysis. After long enough time so that the we can neglect the initial conditions, the mean phenotype at time *t* is

$$\bar{z}_t = S_{tot}G_0 \int_0^{\infty} e^{-S_{tot}G_0 x} \theta_{tot,t-x} dx. \quad \text{(A8)}$$

Equation (A8) is the continuous time equivalent to equation (A6) once the effect of initial conditions has been erased. From equations (A7) and (A8), the method to derive the

autocorrelation of the selection gradient is described in Chevin and Haller (2014, appendix for the autoregressive optimum). This approach cannot a priori be used in the context of the present model because the inflation factor is 1 for $\tau = 0$ and is not defined for $0 < \tau < 1$. However, we found that the naïve approach to use equation (12) in the main text directly in the derivations from Chevin and Haller (2014) matches closely the exact discrete time approach that we develop in the next section. As we could not demonstrate this observation formally, we chose not to present this result in our main text. We nevertheless provide this result here as a heuristic:

$$\rho_{\beta tot,\tau} = \varphi \frac{\rho^{\tau T} - S_{tot} G_0 \frac{T_\theta}{T} e^{-S_{tot} G_0 \tau}}{1 - S_{tot} G_0 \frac{T_\theta}{T}}, \quad \text{(A9)}$$

where $\frac{T_\theta}{T}$ measures the characteristic timescale of the autocorrelation of the environment in units of generation time.

Discrete time approach

In contrast with previous studies (Lande and Shannon 1996, Chevin and Haller 2014), we calculate the autocorrelation of the selection gradient in discrete time. Similarly to the calculation for the variance of the selection gradient, we use equation (A5) assuming that many generations occurred so that the first term can be neglected. We also use equation (12) in the main text for the autocorrelation of the effective optimum $\rho_{\theta tot,\tau} = \rho^{\tau T} \varphi$, reminding that $\varphi = 1$ for $\tau = 0$. The general procedure follows Chevin and Haller (2014, appendix for the autoregressive optimum) by calculating each expectation from equation (A7). Even though we kept notations concise, each sum in the expectations below can be resolved exactly. The first expectation is straightforward

$$\mathrm{E}\left[\theta_{tot,g} \theta_{tot,g-\tau}\right] = \varphi \mathrm{Var}[\theta_{tot}] \rho^{\tau T}. \quad \text{(A10)}$$

The expectation for the first cross product is

836 $\mathrm{E}\left[\bar{z}_{g-\tau}\theta_{tot,g}\right] = S_{tot}G_0 \sum_{i=1}^{g-\tau}(1 - S_{tot}G_0)^{i-1}E\left[\theta_{tot,g}\theta_{tot,g-i-\tau}\right]$, taking into account the

837 discontinuity of the inflation factor I_f in $i = g - \tau$, it results in

838 $E\left[\bar{z}_{g-\tau}\theta_{tot,g}\right] = \varphi\mathrm{Var}[\theta_{tot}]S_{tot}G_0 \sum_{i=1}^{g-\tau-1}(1 - S_{tot}G_0)^{i-1}\rho^{(\tau+i)T} + S_{tot}G_0(1 -$

839 $S_{tot}G_0)^{g-\tau-1}\mathrm{Var}[\theta_{tot}]$. (A11)

840 The expectation for second cross product is

841 $E\left[\theta_{tot,g-\tau}\bar{z}_g\right] = S_{tot}G_0 \sum_{i=1}^{g}(1 - S_{tot}G_0)^{i-1}E(\theta_{tot,g-i}\theta_{tot,g-\tau})$.

842 We need to distinguish 3 cases, $i < \tau$, $i > \tau$ and $i = \tau$:

843 $E\left[\theta_{tot,g-\tau}\bar{z}_g\right] = \varphi\mathrm{Var}[\theta_{tot}]S_{tot}G_0 \left(\sum_{i=1}^{\tau-1}(1 - S_{tot}G_0)^{i-1}\rho^{(\tau-i)T} + \sum_{i=\tau+1}^{g}(1 -\right.$

844 $\left. S_{tot}G_0)^{i-1}\rho^{(i-\tau)T} + \varphi^{-1}(1 - S_{tot}G_0)^{\tau-1}\right)$. (A12)

845 Lastly,

846 $E\left[\bar{z}_g\bar{z}_{g-\tau}\right] = (S_{tot}G_0)^2 \sum_{i=1}^{g}\sum_{k=1}^{g-\tau}(1 - S_{tot}G_0)^{i+k-2}E\left[\theta_{tot,g-i}\theta_{tot,g-\tau-k}\right]$.

847 To calculate the double sum, it is convenient to perform a change of variables

848 $\sum_{i=1}^{g}\sum_{k=1}^{g-\tau}(1 - S_{tot}G_0)^{i+k-2}E\left[\theta_{tot,g-i}\theta_{tot,g-\tau-k}\right] = \sum_{i=1}^{g}\sum_{j=\tau+1}^{g}(1 -$

849 $S_{tot}G_0)^{i+j-\tau-2}E\left[\theta_{tot,g-i}\theta_{tot,g-j}\right]$.

850 We then need to distinguish 4 cases,

851 for $i < \tau+1$, $A = \varphi\mathrm{Var}[\theta_{tot}] \sum_{i=1}^{\tau}\sum_{j=\tau+1}^{g}(1 - S_{tot}G_0)^{i+j-\tau-2}\rho^{(j-i)T}$.

852 for $i > \tau$ and $i = j$, $B = \mathrm{Var}[\theta_{tot}] \sum_{i=\tau+1}^{g}(1 - S_{tot}G_0)^{2i-\tau-2}$.

for $i > \tau$ and $j > i$, $C = \varphi \mathrm{Var}[\theta_{tot}] \sum_{j=\tau+2}^{g} \sum_{i=\tau+1}^{j-1} (1 - S_{tot} G_0)^{i+j-\tau-2} \rho^{(j-i)T}$.

for $i > \tau$ and $i > j$, $D = \varphi \mathrm{Var}[\theta_{tot}] \sum_{i=\tau+2}^{g} \sum_{j=\tau+1}^{i-1} (1 - S_{tot} G_0)^{i+j-\tau-2} \rho^{(i-j)T}$,

with C = D, and resulting in

$$E\left[\bar{z}_g \bar{z}_{g-\tau}\right] = (S_{tot} G_0)^2 (A + B + 2C). \quad \text{(A13)}$$

Adding equations (A10) to (A13), finding the limit of this sum for large *g*, dividing by the variance of the selection gradient (eq. 16) and rearranging leads to the autocorrelation of the selection gradient

$$\rho_{\beta tot,\tau} = \frac{\varphi \varepsilon \rho^{\tau T} + \gamma (1 - S_{tot} G_0)^{\tau}}{\vartheta}, \quad \text{(A14)}$$

where,

$$\varepsilon = (\rho^T - 1)^2 (2 - S_{tot} G_0),$$

$$\gamma = \frac{S_{tot} G_0}{(1 - S_{tot} G_0)} \left(\rho^T (1 - \varphi) (S_{tot} G_0)^2 - (1 - \rho^T) \left(1 + \rho^T (2\varphi - 1)\right) (1 - S_{tot} G_0) \right),$$

$$\vartheta = 2(\rho^T - 1 + S_{tot} G_0)(\rho^T - 1 + \rho^T (\varphi - 1) S_{tot} G_0).$$

Equation (A14) is written in a form similar to equation (A9), decomposing the effects of the autocorrelation of the environment and of the deviations of the mean phenotype to the optimum. An interpretation for equation (A14) is proposed in the main text.

In the special case where there is a unique episode of selection per generation, i.e. $\varphi = 1$, equation (A14) is

$$\rho_{\beta tot,\tau} = \frac{\rho_{\theta}^{\tau T} - \kappa (1 - S_{tot} G_0)^{\tau}}{1 - \kappa}, \quad \text{(A15)}$$

where $\kappa = \frac{(1+\rho^T)S_{tot}\,G_0}{(1-\rho^T)(2-S_{tot}\,G_0)}$.

Equation (A15) is very similar to equation 5b in Chevin and Haller (2014). Comparing equation (A14) and (A15) shows that the inflation factor, i.e. the autocorrelation of selection within generation, complicates the analysis by introducing new terms at the interface between the autocorrelation of the environment and the dynamics of selection within and across generations. A Taylor expansion performed on the reciprocals of equation (A15) and 5b in Chevin and Haller (2014) shows that both equations are identical to at least the second order. This result can be confirmed by representing both functions for different autocorrelation of the environment. Both functions match exactly on most of the autocorrelation range with minor deviation at very weak autocorrelation (not shown).

Changes in (co)variances under selection

Here we derive the changes in the variances and covariances of phenotypic components after each selection episode. Following classical quantitative genetics, we assume that the phenotype z of any individual prior to any selection in a generation is the sum of two normally distributed components: the breeding value x and environmental effect e. At the beginning of a generation, these phenotypic components have means $\bar{x}$ and $\bar{e} = 0$, variances G and E, and are uncorrelated, such that their covariance is $C_{x,e} = 0$ and the total phenotypic variance is $P = G + E$. Changes in the mean breeding value under selection are obtained from changes in mean phenotype using the regression of breeding values on phenotypes, which at the beginning of a generation has slope $\frac{\mathrm{Cov}(x,z)}{P} = \frac{G}{G+E} = h^2$, following the usual notation for heritability.

We consider episodes of selection caused by a Gaussian fitness peak, such that individuals with phenotype z have fitness $(z) \propto \exp(-\frac{(z-\theta)^2}{2\omega^2})$ (where we omit indices for selection episodes and generation for simplicity). It is informative to start by investigating the first selection episode in a generation, where x and e are independent and $\bar{e} = 0$, $\bar{z} = \bar{x}$. The fitness function on breeding values is obtained by integrating over the distribution of environmental effects, $\widetilde{W}(x) \propto \exp\left(-\frac{(x-\theta)^2}{2(\omega^2+E)}\right)$, and the fitness function on environmental effects is obtained similarly by integrating over breeding values, $W_e(e) \propto \exp(-\frac{(\bar{x}+e-\theta)^2}{2(\omega^2+G)})$. The fitness function on breeding values (respectively, on environmental effects) is thus also Gaussian, with squared width $\omega^2 + V_e$ (respectively $\omega^2 + G$) and optimum θ (respectively $\theta - \bar{x}$). With a Gaussian fitness peak, the distribution of phenotypes, breeding values and environmental effects after selection remain Gaussian. Denoting the per-episode strength of stabilizing selection as $S = \frac{1}{\omega^2+P}$, the means after selection are

$$\bar{z}^* = \theta + \frac{\omega^2}{\omega^2+P}(\bar{z} - \theta) = \theta + (1 - SP)(\bar{z} - \theta) = \bar{z} - SP(\bar{z} - \theta) \quad \text{(A16a)}$$

$$\bar{x}^* = \theta + \frac{\omega^2+V_e}{\omega^2+P}(\bar{x} - \theta) = \theta + (1 - SG)(\bar{x} - \theta) = \bar{z} - SG(\bar{z} - \theta) \quad \text{(A16b)}$$

$$\bar{e}^* = \theta - \bar{x} + \frac{\omega^2+G}{\omega^2+P}(\bar{x} - \theta) = \theta - \bar{x} + (1 - SE)(\bar{x} - \theta) = -SE(\bar{z} - \theta)\,, \quad \text{(A16c)}$$

where we have used the fact that $\bar{e} = 0$ and thus $\bar{z} = \bar{x}$ prior to any selection. Note that $\bar{x}^* - \bar{x} = h^2(\bar{z}^* - \bar{z})$ and $\bar{e}^* - \bar{e} = (1 - h^2)(\bar{z}^* - \bar{z})$, as required. The variances after selection are

$$P^* = \left(\frac{1}{\omega^2} + \frac{1}{P}\right)^{-1} = (1 - SP)P \quad \text{(A17a)}$$

$$G^* = \left(\frac{1}{\omega^2+E} + \frac{1}{G}\right)^{-1} = (1 - SG)G \quad \text{(A17b)}$$

910 $$E^* = \left(\frac{1}{\omega^2+G} + \frac{1}{E}\right)^{-1} = (1 - SE)E, \quad \text{(A17c)}$$

911 which satisfy the relationships $G^* - G = h^4(P^* - P)$ and $E^* - E = (1 - h^2)^2(P^* - P)$. The
912 phenotypic variance after selection must also satisfy

913 $$P^* = G^* + E^* + 2\,C^*_{x,e} \quad \text{(A18)}$$

914 so the covariance of breeding values and environmental effects after selection is

915 $$C^*_{x,e} = \frac{P^* - G^* - E^*}{2}. \quad \text{(A19)}$$

916 Using $P = G + E$ this yields

917 $$C^*_{x,e} = \frac{(1-SP)P - (1-SG)G - (1-SE)E}{2} = -S\frac{P^2 - G^2 - E^2}{2} = -SGE, \quad \text{(A20)}$$

918 which satisfies $C^*_{x,e} = C^*_{x,e} - C_{x,e} = h^2(1 - h^2)(P^* - P)$.

919 These formulas apply to the first selection episode, but in further episodes the change in the mean
920 breeding value and environmental effects also depend on their covariance. More general formulas
921 for change at any selection episode can be derived through a multivariate approach. Let us denote
922 the vector of breeding values and environmental effects as $\mathbf{y} = (x, e)^{\mathrm{T}}$ (where superscript T
923 denotes a transposition), with mean $\bar{\mathbf{y}}$ and covariance matrix $\mathbf{Y}$. Substituting $x + e$ for z in the
924 fitness function $W(z)$, and integrating over the joint distribution of x and e, the mean fitness is

925 $$\bar{W} \propto \exp\left(-\frac{S_C\,(\bar{x} + \bar{e} - \theta)^2}{2}\right) \quad \text{(A21)}$$

926 $$S_C = \frac{1}{\omega^2 + G + E + 2C_{x,e}} \quad \text{(A22)}$$

927 Then using standard results from evolutionary quantitative genetics (Lande 1979, 1980, Lande and
928 Arnold 1983) and properties of the Gaussian function, the change in the vector of mean breeding
929 values and environmental effects under selection within a generation is

930 $$\Delta^*\bar{\mathbf{y}} = \mathbf{Y}\partial_{\bar{\mathbf{y}}}\ln\bar{W} \quad \text{(A23)}$$

931 where $\partial_{\bar{\mathbf{y}}}$ is the vector of partial derivatives with respect to each element of $\bar{\mathbf{y}}$, yielding

932 $$\Delta^*\bar{x} = -S_C(\bar{x} + \bar{e} - \theta)(G + C_{x,e}) \quad \text{(A24a)}$$

933 $$\Delta^*\bar{e} = -S_C(\bar{x} + \bar{e} - \theta)(E + C_{x,e}) \quad \text{(A24b)}$$

934 $$\Delta^*\bar{z} = \Delta^*\bar{x} + \Delta^*\bar{e} = -S_C(\bar{x} + \bar{e} - \theta)(G + E + 2C_{x,e}) \quad \text{(A24c)}$$

935 When $\bar{e} = C_{x,e} = 0$, these simplify to $\Delta^*\bar{x} = -SG(\bar{x} - \theta)$ and $\Delta^*\bar{e} = -SE(\bar{x} - \theta)$, consistent
936 with the formulas above for the first episode of selection. The recursion for the covariance matrix
937 is

938 $$\Delta^*\mathbf{Y} = \mathbf{Y}(\partial^2_{\bar{\mathbf{y}}}\ln\bar{W})\mathbf{Y} \quad \text{(A25)}$$

939 where $\partial^2_{\bar{\mathbf{y}}}$ is the Hessian matrix of second partial derivatives with respect to each element of $\bar{\mathbf{y}}$,
940 yielding

941 $$\Delta^*G = -S_C(G + C_{x,e})^2 \quad \text{(A26)}$$

942 $$\Delta^*E = -S_C(E + C_{x,e})^2 \quad \text{(A27)}$$

943 $$\Delta^*C_{x,e} = -S_C(G + C_{x,e})(E + C_{x,e}) \quad \text{(A28)}$$

944 When $\bar{e} = C_{x,e} = 0$, these simplify to $\Delta^*G = -SG^2$, $\Delta^*E = -SE^2$, and $C_{x,e} = -SGE$, again
945 consistent with the formulas above for the first episode of selection.

In the general case where $\bar{e}$ and $C_{x,e}$ are non-zero, as is expected if the population has previously undergone any episode of selection in the ongoing generation, then the relationship between phenotypic change and change in breeding values cannot be inferred directly from current components of phenotypic variance. Indeed we have

$$\frac{\Delta^*\bar{x}}{\Delta^*\bar{z}} = \frac{G+C_{x,e}}{G+E+2C_{x,e}} = \frac{\mathrm{Cov}(x,x+e)}{\mathrm{Var}(x+e)} \qquad \text{(A29)}$$

which is still a regression slope of breeding values on phenotypes, but this no longer translates into a ratio of additive genetic variance on phenotypic variance, because of the covariance between breeding values and environmental values. However, it can be shown that this ratio always equals the ratio $\frac{G}{G+E} = h^2$ at the beginning of a generation.

References

Charlesworth, B. 1993. Directional selection and the evolution of sex and recombination. Genetics Research **61**:205-224.

Chevin, L. M., and B. C. Haller. 2014. The temporal distribution of directional gradients under selection for an optimum. Evolution **68**:3381-3394.

Lande, R. 1979. Quantitative genetic analysis of multivariate evolution, applied to brain: body size allometry. Evolution **33**:402-416.

Lande, R. 1980. Sexual dimorphism, sexual selection, and adaptation in polygenic characters. Evolution **34**:292-305.

Lande, R., and S. J. Arnold. 1983. The measurement of selection on correlated characters. Evolution **37**:1210-1226.

967 Lande, R., and S. Shannon. 1996. The role of genetic variation in adaptation and population
968 persistence in a changing environment. Evolution **50**:434-437.

969

970